Detecting Symmetry in Scalar Fields Using Augmented Extremum Graphs

Supplemental Figures

1. Results on additional cryo-electron microscopy data

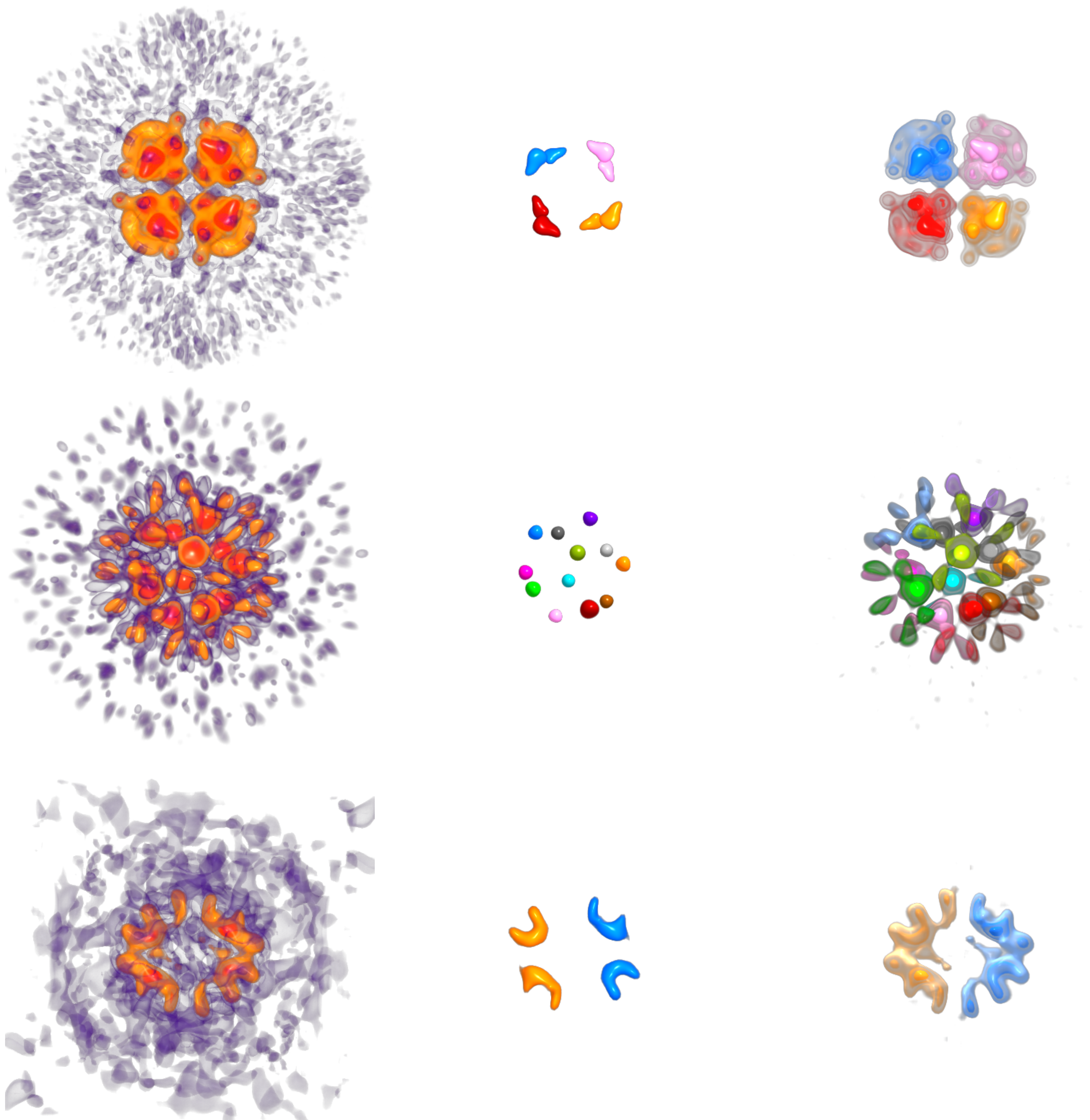

Fig. 1. Symmetry detection results on additional cryo-electron microscopy datasets - EMDB 1319, 1659, and 5215. Each row shows a volume rendering of a dataset, the seed set, and the symmetric regions detected by our method. Each symmetric region is shown in a unique color. The violet regions are representative of the noise in the data. The symmetry detection method works even in the presence of noise.

2. Comparison with the contour tree based method [35]

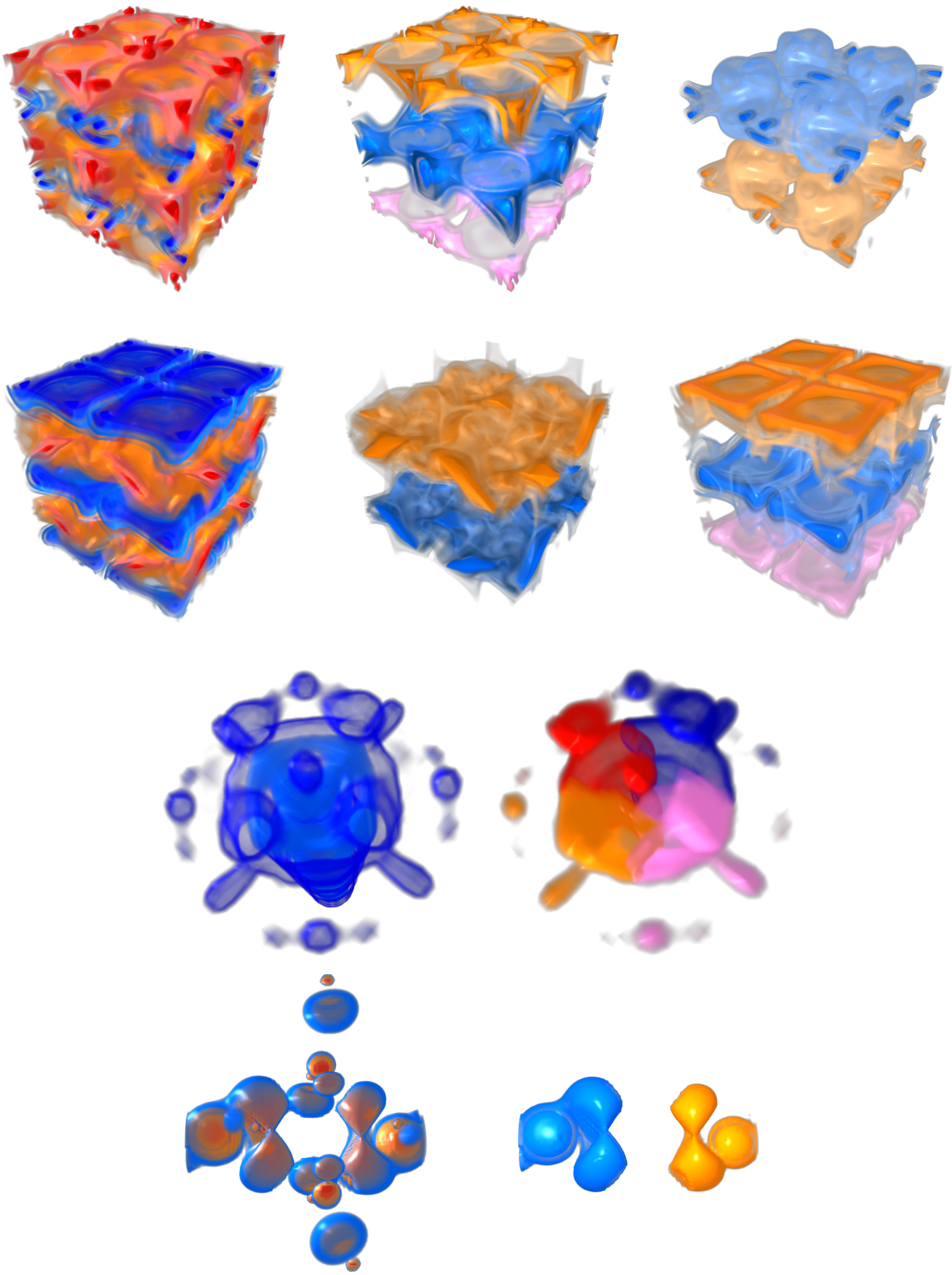

Fig. 2. Advantages of the contour tree method [35]. First and second rows show volume rendering of the two vortex datasets [35] and the symmetries detected by our method using the maximum graph and the minimum graph. Third and fourth row shows the fuel dataset and the neghip dataset and the partial symmetries detected in them. Our method can detect symmetry only at the largest scale whereas the contour tree method can detect symmetries at multiple scales as well as different partial symmetries in the data.

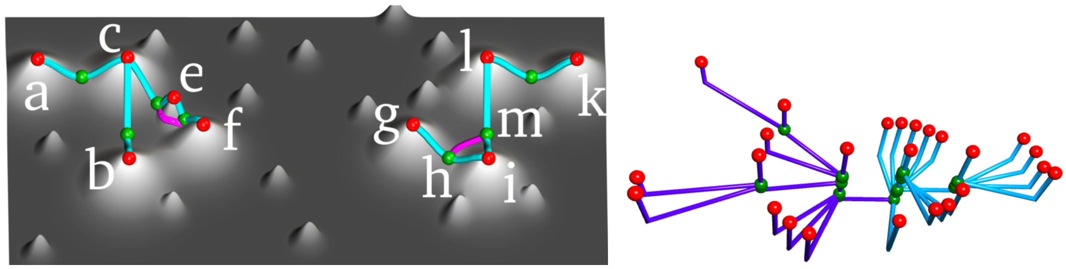

(a) (b)

Fig. 3. Advantages of symmetry detection using augmented extremum graphs compared to symmetry detection using contour trees [35]. The contour tree method fails to detect symmetry when the repeating structure of the branches corresponding to the symmetric regions is destroyed either due to noise or changes in the level set topology. (a) A synthetic terrain dataset where the region on the left and right are symmetric. The distances estimated using the augmented extremum graph is not affected by noise while (b) the noise destroys the repeating structure of the subtrees in the branch decomposition representation. Thus the violet and the blue subtrees corresponding to the symmetric regions on the left and the right are not identified to be repeating and the symmetry is not detected.

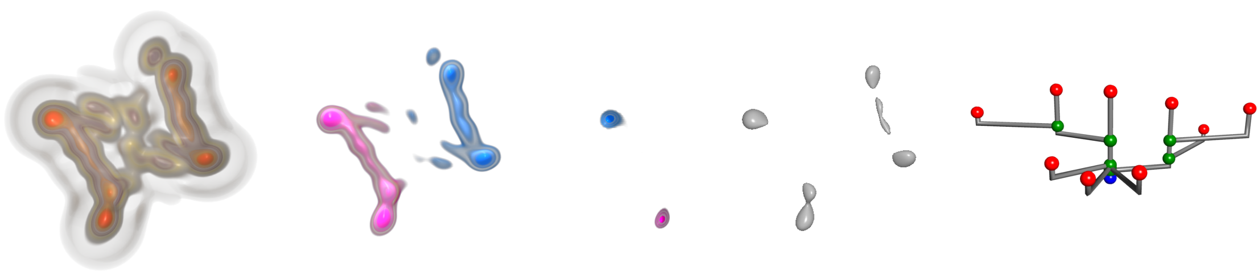

(a) (b) (c) (d) (e)

Fig. 4. A real-world dataset illustrating improved symmetry detection using our method as compared to the contour tree-based method [35]. (a) A dataset (EMDB 5214) with 2-fold rotational symmetry. (b) Our method identifies the global symmetry whereas (c) symmetry detection using contour tree can only identify partial symmetry of two smaller regions. (d) Even though the dataset is symmetric, the level-set components evolve differently and hence (e) the branch decomposition representation of the symmetric regions are also different. In the presence of significant noise, symmetry detection using contour trees perform poorly since the symmetric regions do not manifest as repeating subtrees in the branch decomposition representation. Our method, on the other hand, is not affected by the asymmetric evolution of the level set components since their geometric proximity is captured by the augmented extremum graph and the graph cut correctly partitions them into two symmetric regions.

3. Semi-automatic procedure for seed selection

Fig. 5. Seed selection using toporrery layout. (left) User identifies an extremum of interest and selects the branch corresponding to it from the toporrery layout. The selected branch is shown in orange and other branches whose extrema have function values similar to extrema of the selected branch are automatically selected and shown in blue. (middle) User inspects the level sets of the selected branches. Among the sixteen branches selected, the evolution of the level sets corresponding to eight of the branches are similar and (right) the user selects this subset of branches shown in orange. The extrema corresponding to the selected branches are chosen as the seed set.

4. Sensitivity to seed set selection

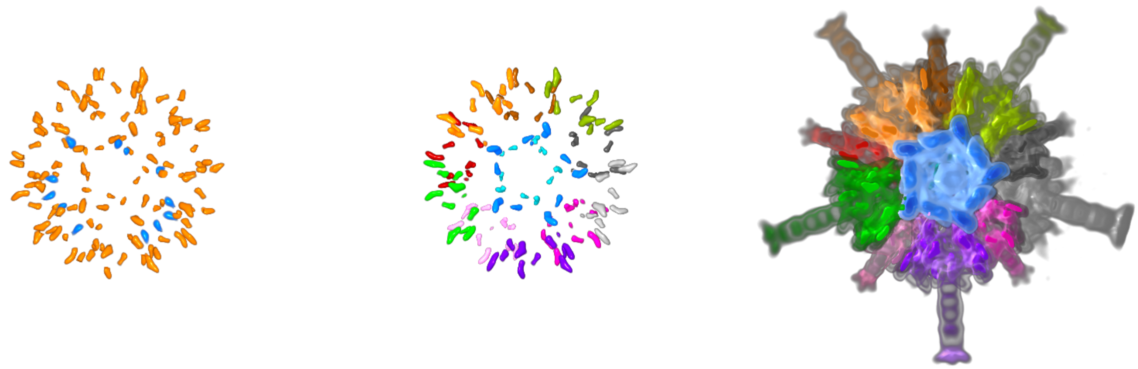

Fig. 6. Effect of insertion of seeds to the ideal seed set. (left) New seeds shown in blue are inserted into the ideal seed set shown in orange. (middle) Despite the asymmetric distribution of seeds, they form super-seeds that represent the symmetry in the data and (right) the symmetric regions are detected correctly.

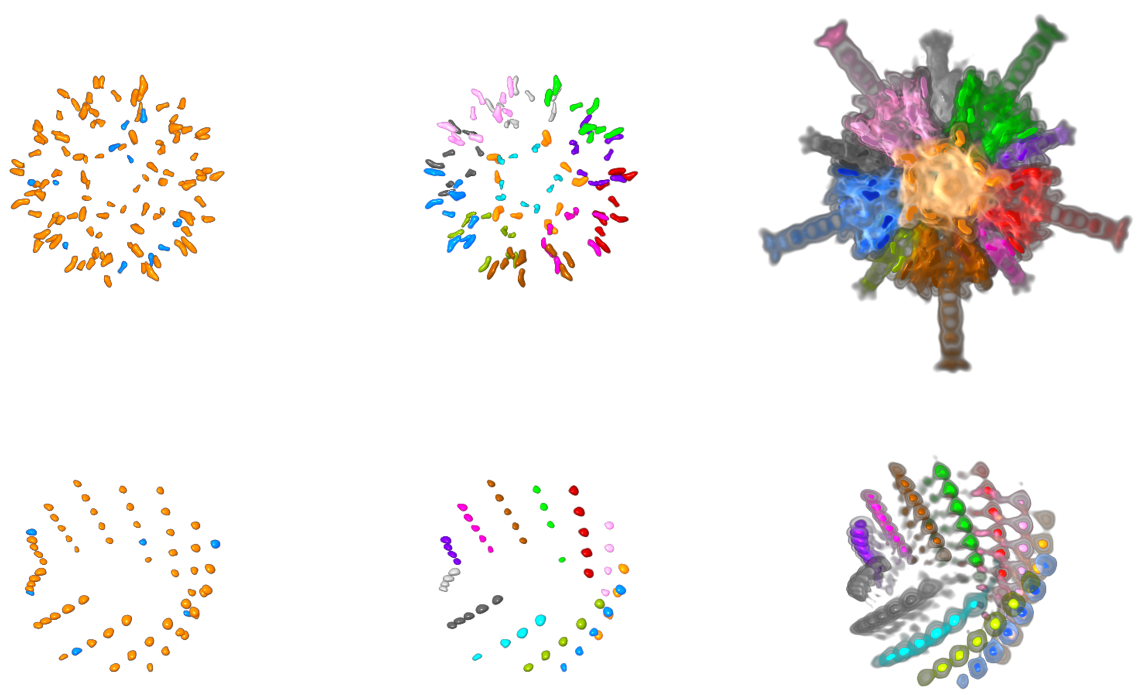

Fig. 7. Effect of deletion of seeds from the ideal seed set. (left) Seeds shown in blue are removed from the ideal seed set and the remaining seeds are shown in orange. (middle) Despite removal of seeds, the super-seeds are formed correctly and (right) the symmetric regions are detected.

Fig. 8. Effect of both insertion and deletion of seeds from the ideal seed set. (left) From the ideal seed set, (middle) five new seeds are inserted and two seeds are removed. The super-seeds formed represent the symmetry in the data and (right) the symmetric regions are detected correctly.

5. Symmetry detection with different noise levels

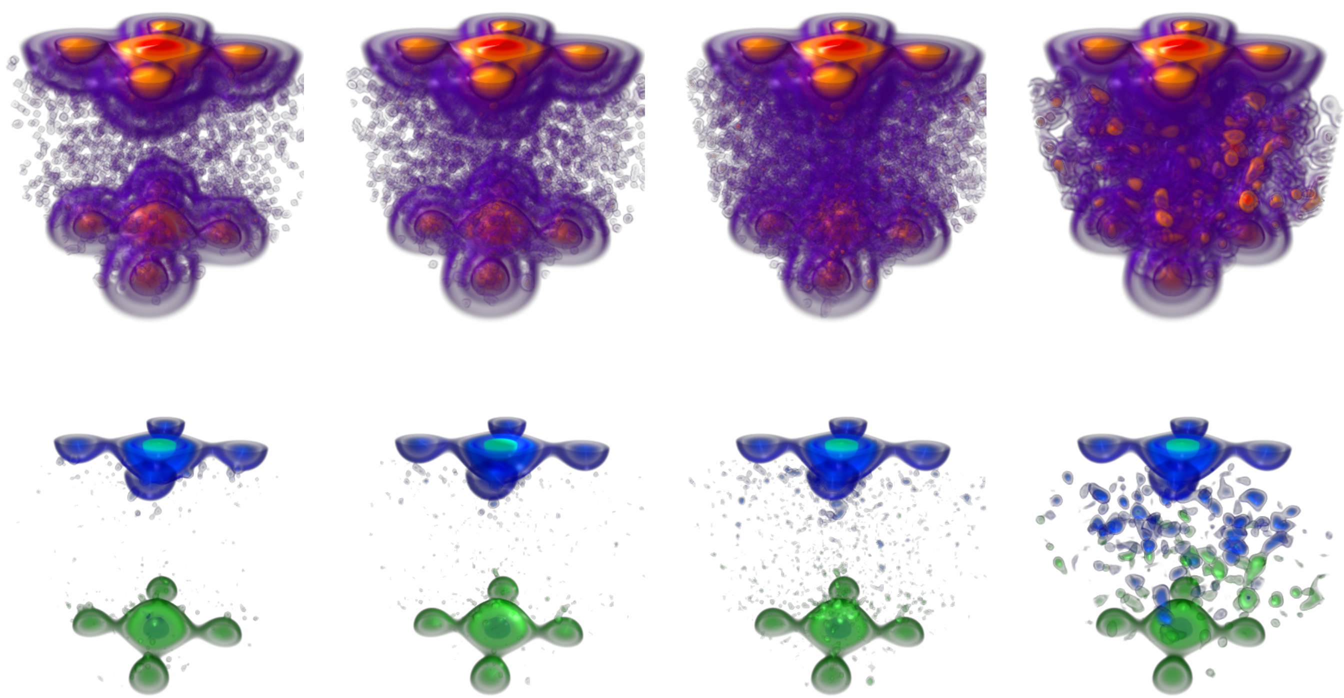

Fig. 9. Our symmetry detection method is robust in the presence of noise. (top) A synthetic dataset with increasing levels of noise is shown from left to right. The transfer function used is identical in each case and shows the increasing levels of noise. (bottom) The symmetric regions detected are shown in blue and green in the bottom row.

6. Parameter selection plots

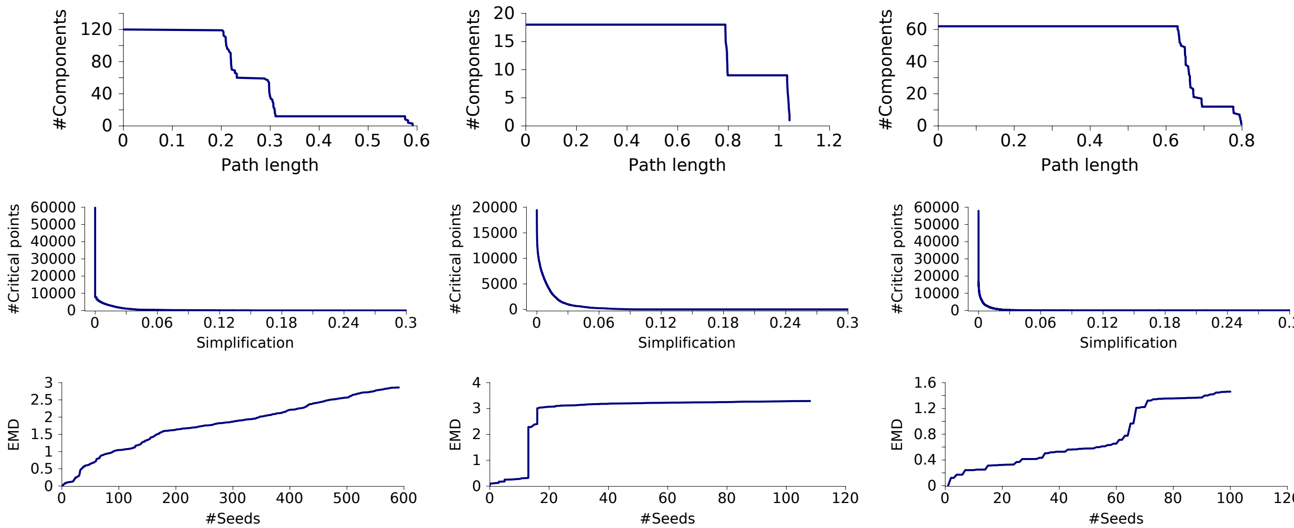

Fig. 10. Plots for the selection of parameters for the datasets EMDB 1179, 1603, and 5331. The first row shows the plot of the number of components with path length and the stable horizontal interval that is leftmost is used to identify the threshold for disconnecting the seed-merge tree. The second row shows the plot of the number of extrema with simplification and the start of the horizontal section where the curve tapers off is used to select the threshold for simplification. The third row shows the plot of the number of seeds with EMD. The threshold for identifying seeds is chosen from the nearly vertical sections in the plots. The plot for the dataset EMDB 1179 does not have a clear vertical section and hence is not used for seed selection while the threshold of 0.9 used for the remaining two datasets lies in the vertical section.

7. Plots used for identifying super-seeds from asymmetric seed set

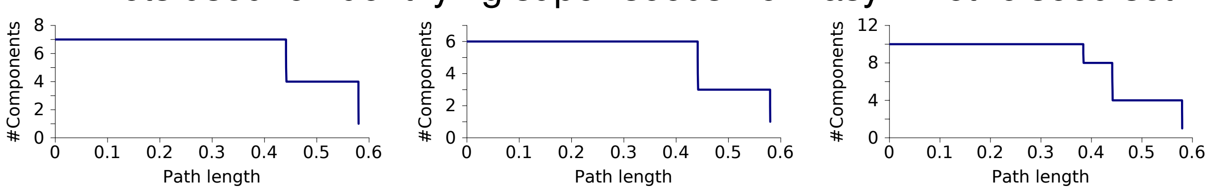

Fig. 11. Plots used for identifying super-seeds when seed sets that differ from the ideal seed set is used for the dataset EMDB 1654. The figure shows the plot (left) when one seed is dropped, (middle) both seeds are dropped, and (right) two new seeds are inserted. In all cases, the super-seeds are identified by choosing a threshold that lies in the leftmost horizontal interval.